UDC 539.3

N. D. Vaysfeld[1], Z. Yu. Zhuravlova[2]✉

RESPONSE OF A POROELASTIC SEMI-INFINITE STRIP TO THE COMPRESSION ACTING UPON ITS LATERAL SIDES

A mixed boundary value problem for a poroelastic semi-infinite strip is formulated using Biot's theory. Two cases of boundary conditions are considered depending on the permeability of the longer sides. By using the integral transforms and matrix differential calculus, the original boundary value problem was reduced to a one-dimensional one, which then is solved analytically. The explicit formulae are derived for the effective stress, pore pressure, and displacements. These functions are analyzed depending on the permeability of the boundary, the properties of poroelastic material, and the compression profile along the sides.

Key words: *poroelastic semi-strip, integral transform, matrix differential calculus, vector boundary problem, exact solution.*

Introduction. The mechanical performance of poroelastic materials is a relevant scientific challenge due to the numerous applications. The poroelastic models can cover various engineering applications, such as construction, biomechanics, chemical, petrochemical, and geological industries, etc. In particular, the problem of poroelasticity for a rectangular domain can be regarded as a benchmark problem for groundwater reservoirs as relatively isolated extended water-saturated rock layers.

The foundations of the poroelasticity theory were laid by Terzaghi [16] and Biot [7]. Various numerical and analytical methods for solving problems within the framework of this theory have been developed since. The boundary element and variational methods can be regarded as the dominant ones concerning the numerical mode of attack. The boundary element method was used in [10] for studying the dynamic response of an embedded strip and shallow rectangular foundations subjected to time-harmonic vertical excitation. The vertical vibrations of an assembly of flexible strip foundations resting upon multilayered transversely isotropic poroelastic soils were addressed in [20]. The dynamic interaction problem was studied by employing a variational approach based on the discretization of the strip − soil contact area. Numerical methods, however, fail to provide a complete qualitative picture, which can be obtained through the analytical approaches.

The dynamic response of a rectangular poroelastic plate to the harmonic loading was analyzed in [17] using an analytical-numerical procedure based on the Fourier double series for the case when the plate is simply supported, thin, and fluid-saturated. A plane contact problem of interaction between a rigid punch and an elastic strip bonded to a poroelastic half-plane was considered in [8]. The deformation of the half-plane was modeled on the basis of the Cowin − Nunziato equations for poroelastic solids. Using the integral Fourier transform, the problem was reduced to a singular integral equation for the unknown contact stress. This equation was solved by the collocation method. The study of dynamic response of a multi-layered poroelastic half-plane was outlined in [19] by adopting an exact stiffness matrix method. A semi-analytical discretization scheme (based on the obtained fundamental solutions) was employed to investigate the dynamic response of a rigid strip foundation bonded to poroelastic soils. A problem on the indentation of a half-space with Biot poroelastic properties was examined in [18]. The mixed initial-boundary-value problems associated with the adhesive-impermeable indentation were reduced to a set of coupled Fredholm integral equations of the second kind in the Laplace transform domain. A coupled model was proposed in [12] to study the

─────────────────

✉ z.zhuravlova@onu.edu.ua

effect of dynamic water pressure caused by the strip vibration in the offshore foundations. The solution to the strip vibration problem was obtained there by an integral equation method. The results were expressed in terms of dual integral equations converted into Fredholm integral equations, which then are solved numerically.

A problem of plane-strain poroelasticity induced by surface-normal loading within a finite rectangular fluid-saturated domain was solved analytically in [14]. The investigation of the three-dimensional wave propagation in a poroelastic plate immersed in an inviscid elastic fluid was performed in [21]. An analytical method comprising the transformation of the mixed boundary conditions to dual integral equations, which are solved by means of the Jacobi orthogonal polynomials, was presented in [25] to determine the response of rigid strip footings to harmonic horizontal loads while considering the foundation soil as a poroelastic two-phase medium. An analytical solution was obtained in [22] for the coupled diffusion−deformation system of equations governing the quasi-static plane deformation of a poroelastic half-space with anisotropic permeability and compressible constituents. The methods for the determination of physical constants in porous liquid-saturated media were analyzed in [2] basing on static and quasistatic methods of measurements with regard to the initial stresses in the material. The methods of irreversible thermomechanics and functional analysis were used in [15] to formulate a mathematical model of a thermoelastic solid taking into account the structural heterogeneity of the material and the geometric irregularity of its surface. It was shown that the model was appropriate to describe coupled processes in porous and nanoporous bodies. Some classical methods of elasticity and rheology can be developed for use in solving poroelasticity problems [3, 5, 6, 13].

Evidently, there are quite a few exact solutions to boundary value problems of poroelasticity. The mutual application of the integral transforms method, and matrix differential calculation made it possible to derive the exact analytical solutions of poroelasticity problems for a semi-plane [23]. An application of this method is demonstrated herein by deriving an exact solution to the poroelasticity problem for a compressed semi-infinite strip.
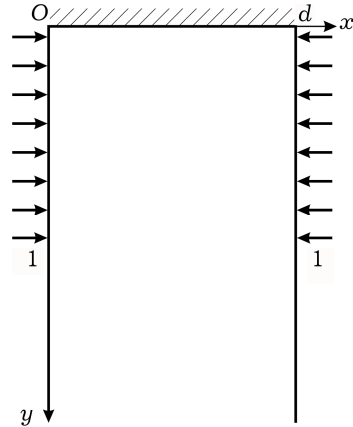
Fig. 1

1. Formulation of the problem. Consider a poroelastic semi-strip $0 < x < d$, $0 < y < \infty$, where $d = a / h$, a is the width of the semi-strip, and h is a characteristic length (presumably, the length of the loading zone, see Fig. 1), within the framework of the Biot model [7]. The boundary conditions on the sides $x = 0$ and $x = d$ cover the following two cases:

i) both mechanical and fluid-pressure loadings are applied, as follows:

$$\sigma_x^F(0, y) = -L_1(y), \qquad \tau_{xy}^F(0, y) = T_1(y), \qquad p(0, y) = P_1(y),$$

$$\sigma_x^F(d, y) = -L_2(y), \qquad \tau_{xy}^F(d, y) = T_2(y), \qquad p(d, y) = P_2(y); \qquad (1)$$

ii) the side $x = 0$ is subject to the mechanical and fluid-pressure loadings, while the side $x = d$ is subject to the mechanical loading under the undrained conditions:

$$\sigma_x^F(0, y) = -L_1(y), \qquad \tau_{xy}^F(0, y) = T_1(y), \qquad p(0, y) = P_1(y),$$

$$\sigma_x^F(d, y) = -L_2(y), \qquad \tau_{xy}^F(d, y) = T_2(y), \qquad \frac{\partial p(d, y)}{\partial x} = 0. \qquad (2)$$

200

Here, $0 < y < 1$, $\sigma_x^F(x,y) = \tilde{\sigma}_x^F(x,y) / G$, $\tau_{xy}^F(x,y) = \tilde{\tau}_{xy}^F(x,y) / G$, $\tilde{\sigma}_{xx}^F(x,y)$ and $\tilde{\tau}_{xy}^F(x,y)$ are the normal and shear stresses, $p(x,y) = \tilde{p}(x,y) / G$, $\tilde{p}(x,y)$ is the pore pressure, G stands for the shear modulus. Note that the given functions $L_\ell(y)$, $T_\ell(y)$, $P_\ell(y)$, $\ell = 1,2$, are equal to zero for $y > 1$.

Conditions (1) and (2) can be rewritten using the relations between the total and effective stresses [24]

$$\sigma_x(0,y) = -L_1(y) - \alpha P_1(y), \quad \tau_{xy}(0,d) = T_1(y), \quad p(0,y) = P_1(y),$$

$$\sigma_x(d,y) = -L_2(y) - \alpha P_2(y), \quad \tau_{xy}(d,y) = T_2(y), \quad p(d,y) = P_2(y), \quad (3)$$

and

$$\sigma_x(0,y) = -L_1(y) - \alpha P_1(y), \quad \tau_{xy}(0,y) = T_1(y), \quad p(0,y) = P_1(y),$$

$$\sigma_x(d,y) = -L_2(y) - \alpha P_2(y), \quad \tau_{xy}(d,y) = T_2(y), \quad \frac{\partial p(d,y)}{\partial x} = P_2(y), \quad (4)$$

where $\sigma_x(x,y)$ and $\tau_{xy}(x,y)$ are the dimensionless normal and shear effective stresses, and α is the Biot coefficient.

Side $y = 0$ is assumed to be impermeable under the following conditions:

$$v(x,0) = 0, \quad \tau_{xy}(x,0) = 0, \quad \frac{\partial p(0,y)}{\partial y} = 0, \quad (5)$$

where $v(x,y) = u_y(x,y) / h$ is the dimensionless displacement of the solid skeleton.

The equilibrium and storage equations can be formulated in the following dimensionless form [24]:

$$\frac{\partial^2 u}{\partial x^2} + \frac{\ae - 1}{\ae + 1}\frac{\partial^2 u}{\partial y^2} + \frac{2}{\ae + 1}\frac{\partial^2 v}{\partial x \partial y} - \alpha \frac{\ae - 1}{\ae + 1}\frac{\partial p}{\partial x} = 0,$$

$$\frac{\partial^2 v}{\partial x^2} + \frac{\ae + 1}{\ae - 1}\frac{\partial^2 v}{\partial y^2} + \frac{2}{\ae - 1}\frac{\partial^2 u}{\partial x \partial y} - \alpha \frac{\partial p}{\partial y} = 0,$$

$$\frac{\partial^2 p}{\partial x^2} + \frac{\partial^2 p}{\partial y^2} - \frac{\alpha}{K}\left(\frac{\partial u}{\partial x} + \frac{\partial v}{\partial y}\right) - \frac{S_P}{K} p = 0. \quad (6)$$

Here, $\ae = 3 - 4\mu$ is the Muskhelishvili constant, μ is Poisson's ratio, S_p is the storativity of the pore volume, k is the permeability coefficient, $K = h^2/(Gk)$, and $S_P = S_p G$.

The stresses, pore pressure, and displacements within the considered semi-infinite domain are to be found from the formulated boundary value problem (3) − (6).

2. Construction of an exact solution. By making use of the semi-infinite sine and cosine Fourier transforms

$$\begin{Bmatrix} u_\beta(x) \\ v_\beta(x) \\ p_\beta(x) \end{Bmatrix} = \int\limits_0^\infty \begin{Bmatrix} u(x,y)\cos\beta y \\ v(x,y)\sin\beta y \\ p(x,y)\cos\beta y \end{Bmatrix} dy,$$

the boundary value problem (3) − (6) can be reduced to a one-dimensional problem in the transform domain

$$u_\beta''(x) + \frac{2\beta}{\ae + 1} v_\beta'(x) - \beta^2 \frac{\ae - 1}{\ae + 1} u_\beta(x) - \alpha \frac{\ae - 1}{\ae + 1} p_\beta'(x) = 0,$$

$$v''_\beta(x) - \frac{2\beta}{x-1} u'_\beta(x) - \beta^2 \frac{x+1}{x-1} v_\beta(x) + \alpha\beta p_\beta(x) = 0 \,,$$

$$p''_\beta(x) - \frac{\alpha}{K} u'_\beta(x) - \frac{\alpha}{K} v_\beta(x) - \left(\beta^2 + \frac{S_P}{K}\right) p_\beta(x) = 0 \,,$$

$$(1-\mu)u'_\beta(0) + \mu\beta v_\beta(0) = \frac{1-2\mu}{2}\left(\alpha P_{1,\beta} - L_{1,\beta}\right) ,$$

$$v'_\beta(0) - \beta u_\beta(0) = T_{1,\beta}, \qquad p_\beta(0) = P_{1,\beta} \,,$$

$$(1-\mu)u'_\beta(d) + \mu\beta v_\beta(d) = \frac{1-2\mu}{2}\left(\alpha P_{2,\beta} - L_{2,\beta}\right) ,$$

$$v'_\beta(d) - \beta u_\beta(d) = T_{2,\beta}, \qquad p_\beta(d) = P_{2,\beta} \,. \tag{7}$$

Here, $P_{\ell,\beta}$, $L_{\ell,\beta}$, and $T_{\ell,\beta}$, $\ell = 1,2$, are the images of functions $P_\ell(y)$, $L_\ell(y)$, $T_\ell(y)$ in the mapping domain of the foregoing sine and cosine transforms.

Formulation (7) can be given [1] in the following vector form:

$$\mathbf{L}_2 \mathbf{y}_\beta(x) = \mathbf{0}, \qquad 0 < x < 1\,,$$

$$\mathbf{A}_\beta \mathbf{y}'_\beta(0) + \mathbf{B}_\beta \mathbf{y}'_\beta(0) = \mathbf{g}_{1,\beta}\,,$$

$$\mathbf{A}_\beta \mathbf{y}'_\beta(d) + \mathbf{B}_\beta \mathbf{y}'_\beta(d) = \mathbf{g}_{2,\beta}\,. \tag{8}$$

Here, $\mathbf{L}_2$ is the second-order operator $\mathbf{L}_2 \mathbf{y}_\beta(x) = \mathbf{I}\mathbf{y}''_\beta(x) - \mathbf{Q}_\beta \mathbf{y}'_\beta(x) - \mathbf{P}_\beta \mathbf{y}_\beta(x)$, $\mathbf{I}$ is the unit matrix, $\mathbf{y}_\beta(x) = \left(u_\beta(x), v_\beta(x), p_\beta(x)\right)^\top$, $\top$ marks the vector transposition, and matrices $\mathbf{Q}_\beta$, $\mathbf{P}_\beta$, $\mathbf{A}_\beta$, and $\mathbf{B}_\beta$, and vectors $\mathbf{g}_{\ell,\beta}$, $\ell = 1,2$, are given in **Appendix**.

A solution to the vector-form boundary-value problem (8) can be derived by using the matrix differential calculation [4], which yields

$$\mathbf{L}_2 \mathbf{Y}_\beta(x) = 0, \qquad 0 < x < 1\,, \tag{9}$$

where $\mathbf{Y}_\beta(x) = \exp(\xi x)\mathbf{I}$. Substituting (9) into (8) yields the equality $\mathbf{L}_2 \exp(\xi x)\mathbf{I} = \mathbf{M}(\xi)\exp(\xi x)$, where

$$\mathbf{M}(\xi) = \begin{pmatrix} \xi^2 - \dfrac{x-1}{x+1}\beta^2 & \dfrac{2\beta}{x+1}\xi & -\alpha\dfrac{x-1}{x+1}\xi \\[2ex] -\dfrac{2\beta}{x-1}\xi & \xi^2 - \dfrac{x+1}{x-1}\beta^2 & \alpha\beta \\[2ex] -\dfrac{\alpha}{K}\xi & -\dfrac{\alpha\beta}{K} & \xi^2 - \beta^2 - \dfrac{S_P}{K} \end{pmatrix}.$$

According to [11], a solution to the homogenous matrix equation is constructed by using the formula

$$\mathbf{Y}(x) = \frac{1}{2\pi i} \oint_C \exp(\xi x)\mathbf{M}^{-1}(\xi)d\xi\,,$$

where $\mathbf{M}^{-1}(\xi)$ is the inverse matrix to $\mathbf{M}(\xi)$, C is a closed contour that covers all singular points of the matrix $\mathbf{M}^{-1}(\xi)$, and i is the imaginary unit.

The determinant of matrix $\mathbf{M}(\xi)$ has two second-order multiple poles $\xi = \pm\beta$, and two single poles $\xi = \pm\sqrt{\beta^2 + \dfrac{S_P}{K} + \dfrac{\alpha^2}{K}\dfrac{x-1}{x+1}}$. With the help of the

202

residual theorem, the system of four fundamental matrix solutions $\mathbf{Y}_j(x)$, $j = 1, 2, 3, 4$, is derived in correspondence to the foregoing eigenvalues.

Hence, a general solution to the problem (8) takes the following form:

$$\mathbf{y}_\beta(x) = \left(\mathbf{Y}_1(x) + \mathbf{Y}_3(x)\right)\begin{pmatrix} c_1 \\ c_2 \\ c_3 \end{pmatrix} + \left(\mathbf{Y}_2(x) + \mathbf{Y}_4(x)\right)\begin{pmatrix} c_4 \\ c_5 \\ c_6 \end{pmatrix}, \qquad (10)$$

where constants c_j are found from the boundary conditions (8), $j = 1, 2, \ldots, 6$.

Solution (10) can be reconstructed in the physical domain by making use of the following inverse transforms:

$$\begin{Bmatrix} u(x, y) \\ v(x, y) \\ p(x, y) \end{Bmatrix} = \frac{2}{\pi} \int_0^\infty \begin{Bmatrix} u_\beta(x)\cos\beta y \\ v_\beta(x)\sin\beta y \\ p_\beta(x)\cos\beta y \end{Bmatrix} d\beta.$$

In such manner, an exact solution of the formulated problem is found in the explicit form. The convergence of the derived integrals was analyzed and numerical calculations were carried out in order to establish the patterns of stress and pressure distribution depending on semi-strip's width, the value of Biot's coefficient and the loading profile.

3. Numerical examples and discussion. Three different case studies are considered regarding the loading on the side $x = 0$:

1) concentrated normal mechanical load $L_1(y) = L_0\delta(y - 1/2)$, $T_1(y) = 0$, $P_1(y) = 0$, where $\delta(y)$ is the Dirac delta-function;

2) distributed normal mechanical load $L_1(y) = L_0\sin\pi y$, $T_1(y) = 0$, $P_1(y) = 0$;

3) distributed fluid pressure $L_1(y) = 0$, $T_1(y) = 0$, $P_1(y) = L_0\sin\pi y$.

In what follows, the dimensional multiplayer L_0 is dropped and the results are presented in the dimensionless form.

Consider three different poroelastic materials with properties given in Table 1. All the figures below demonstrate the distributions of the normal stress σ_x and pore pressure p at $x = d/2$ and $0 < y < 1$. The effect of loadings applied to side $x = d$ in the normal stress and pore pressure within the semi-strip is also analyzed numerically.

Table 1. The characteristics of poroelastic materials [9].

Properties / Material	$G \times 10^{-9}$ [N/m^2]	μ	α	$k \times 10^{13}$ [m^4/(N×s)]	$S_p \times 10^{13}$ [m^2/N]
1 Charcoal granite	18.7	0.27	0.242	0.001	137.7
2 Ruhr sandstone	13.3	0.12	0.637	2.0	260.4
3 Boise sandstone	4.2	0.15	0.853	8.0	2.075

3.1. The case of concentrated normal mechanical load. The permeability of the side $x = d$ affects significantly the pore pressure on this side, while the normal stress and pore pressure vary insignificantly. The largest absolute values of normal stress and pore pressure are observed when approaching the meridian, where the concentrated load is applied. The absolute values of normal stress and pore pressure are greater for the case with an impermeable boundary $x = d$. The response of different porous materials of semi-strip on the compression is shown at Fig. 2 and Fig. 3. The numbers of curves in all the figures correspond to the numbering of materials in Table 1.
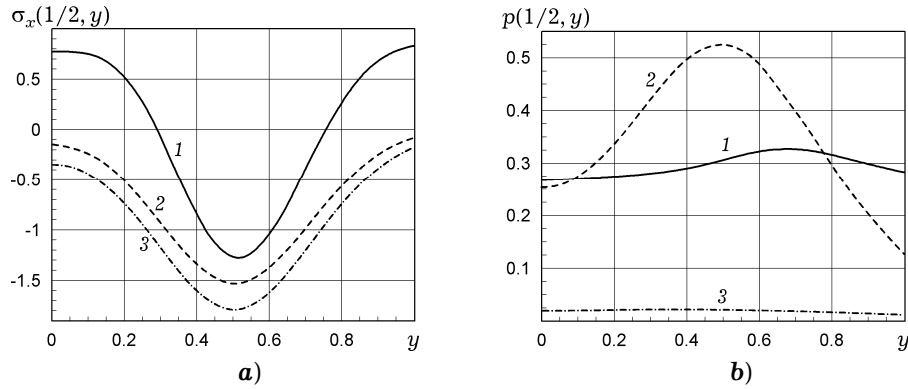
Fig. 2. Distributions of the dimensionless effective stress and pore pressure in the semi-strip for different poroelastic materials under the concentrated normal mechanical loading $L_1(y) = L_2(y) = \delta(y - 1/2)$ with side $x = d = 1$ being permeable.
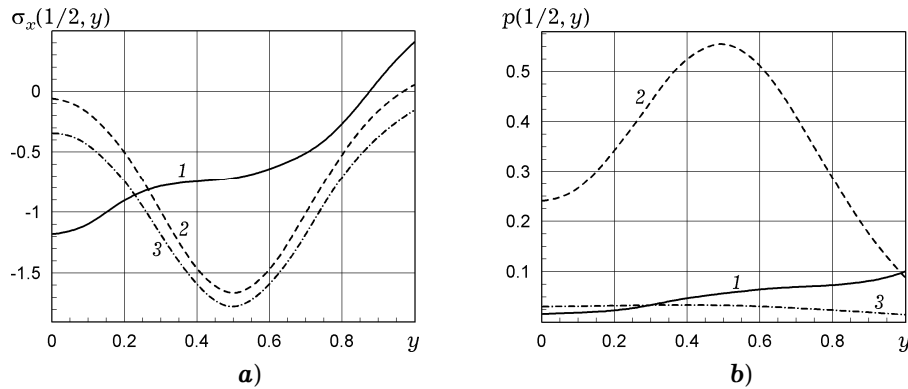
Fig. 3. The functions indicated in Fig. 2 with side $x = d = 1$ being impermeable.

The numerical analysis shows that the higher are the values of Biot's coefficient, the greater absolute values of the normal stress are attained, and the lower pore pressure is observed. This conclusion holds for side $x = d$ being either impermeable or permeable.

3.2. The case of distributed normal mechanical load. As it was stated in the previous case for the concentrated mechanical loading, the same dependences are observed here: the pore pressure depends significantly on the permeability of the lateral side whereas the normal stress remains approximately the same. The tensile stress is observed nearer to the ends of loaded segment for both cases.
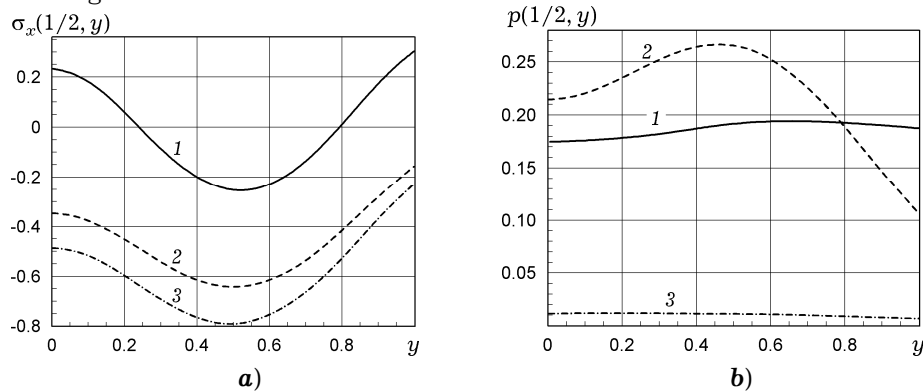
Fig. 4. Distributions of the dimensionless effective stress and pore pressure in the semi-strip for different poroelastic materials under the distributed normal mechanical loading $L_1(y) = L_2(y) = \sin \pi y$ with side $x = d = 1$ being permeable.
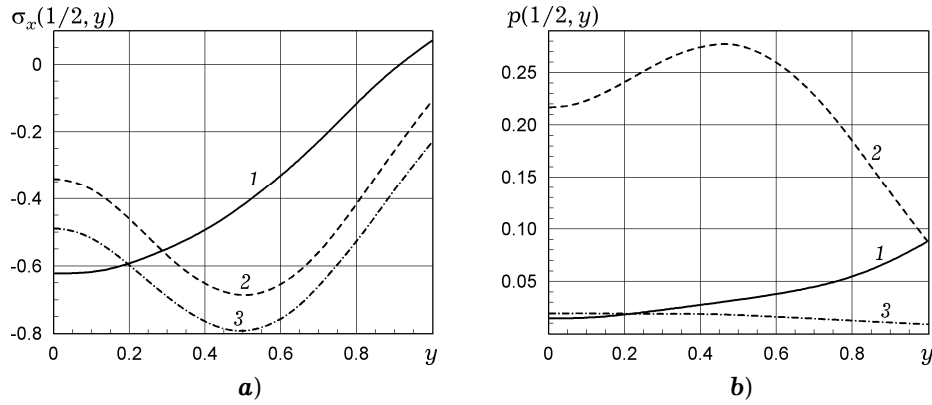
Fig. 5. The functions indicated in Fig. 4 with side $x = d = 1$ being impermeable.

By comparing the situation for this type of load and the case of the considered concentrated mechanical load, one can notice that the absolute values of normal stress and pore pressure in this case are lower than in the case of a concentrated load. The peaks of normal stress and pore pressure are observed near the central point of the applied load. Pore pressure is positive for both cases. The different porous materials were investigated under the distributed mechanical loading impact (see Fig. 4 and Fig. 5).

The distribution of normal stress and pore pressure is analogous to the case of a concentrated load illustrated above. The maximum absolute values of the normal stress and minimum ones of the pore pressure are observed for the material with the highest Biot coefficient.

3.3. The case of distributed fluid pressure load. In general, the distribution patterns of stress and pore pressures are similar to the results given in subsections 4.1 and 4.2. As before, the general trend of the dependence of normal stress and pore pressure on permeability remains the same. However, in contrast to the cases of distributed and concentrated mechanical loads applied to the lateral side, it is noted that both the pressure and the absolute values of the normal stress are greater for the material with higher Biot's coefficient (see Fig. 6 and Fig. 7).

The exact solutions derived in an explicit form make it possible to conduct various numerical investigations of both mechanical characteristics (stresses, displacements) and pore pressure depending on many factors such as the value of Biot's coefficient, permeability conditions on the lateral sides, etc. The analysis of the impact of the load type and the material's porosity revealed the main trends in the change in the hydroelastic state of the semi-strip under various specified boundary conditions.
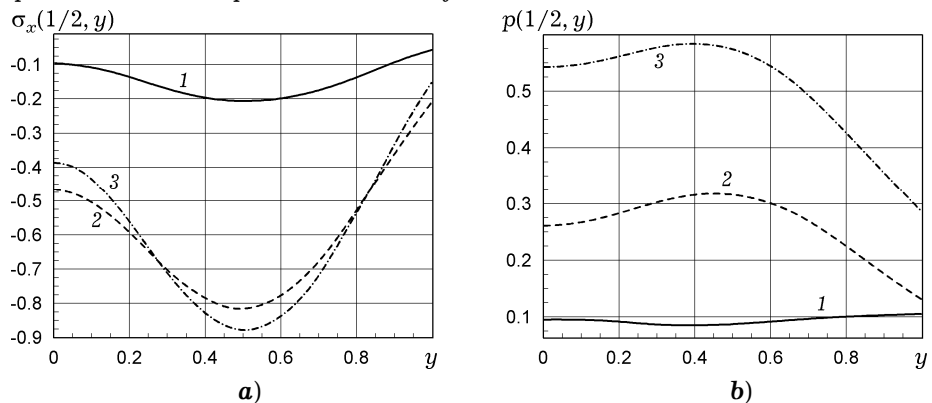
Fig. 6. The distributions of the dimensionless effective stress and pore pressure in the semi-strip for different poroelastic materials under the fluid pressure load $P_1(y) = P_2(y) = \sin \pi y$ with a loaded surface $x = d = 1$.

205
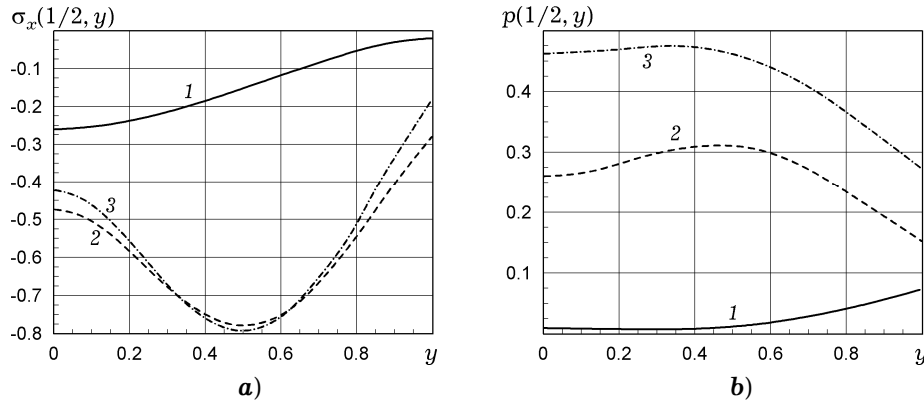
Fig. 7. The functions indicated in Fig. 6 with an impermeable surface $x = d = 1$.

The provided analysis showed that for all types of loads the maximum absolute values of the normal stress and the pore pressure are observed when the width of the semi-strip is smaller than the loaded segment. With the increment of the width the absolute values of the stress and the pore pressure become smaller under the fixed loading for different types of permeability.

The higher is the value of Biot's coefficient, the higher are the absolute values of the normal stress under the influence of all types of loads on both lateral sides under different conditions of permeability of the right side. A similar trend in the pore pressure change with a change of Biot's coefficient is noted in the case when fluid pressure load is set on the left side, and the right side is either loaded with fluid pressure load or is impermeable.

For all types of porous materials, the highest stress and pore pressure values are observed for the concentrated normal mechanical load while their lowest values are registered for the distributed normal mechanical load.

For the case $\alpha = 0$, the results comply with the ones for pure elasticity problems for a semi-strip under the same mechanical conditions.

Conclusions. An exact solution of the poroelastic problem for a semi-infinite strip is derived by a new analytical approach, which is based on integral transform method and matrix differential calculation apparatus. The explicit formulas for the stress and the pore pressure allowed to provide versatile numerical studies of the poroelastic stress state of the semi-strip depending on various factors. An analysis of the numerical results revealed regularities in the distribution of stress and pore pressure depending on the width of the semi-strip, the value of Biot's coefficient of the poroelastic material, and the type of the applied load. The proposed approach can be used for the solving of uncoupled thermoporoelasticity problems for rectangular domains.

Appendix. The matrices and vectors in **(8)**:

$$
\mathbf{Q}_\beta = \begin{pmatrix} 0 & -\dfrac{2\beta}{\mathit{x}+1} & \alpha\dfrac{\mathit{x}-1}{\mathit{x}+1} \\[2mm] \dfrac{2\beta}{\mathit{x}-1} & 0 & 0 \\[2mm] \dfrac{\alpha}{K} & 0 & 0 \end{pmatrix}, \quad \mathbf{P}_\beta = \begin{pmatrix} \beta^2\dfrac{\mathit{x}-1}{\mathit{x}+1} & 0 & 0 \\[2mm] 0 & \beta^2\dfrac{\mathit{x}+1}{\mathit{x}-1} & -\alpha\beta \\[2mm] 0 & \dfrac{\alpha\beta}{K} & \beta^2+\dfrac{S_P}{K} \end{pmatrix},
$$

$$\mathbf{A}_{\beta} = \begin{pmatrix} 1-\mu & 0 & 0 \\ 0 & 1 & 0 \\ 0 & 0 & 0 \end{pmatrix}, \quad \mathbf{B}_{\beta} = \begin{pmatrix} 0 & \beta\mu & 0 \\ -\beta & 0 & 0 \\ 0 & 0 & 1 \end{pmatrix},$$

$$\mathbf{g}_{\ell,\beta} = \frac{1}{2G} \begin{pmatrix} (1-2\mu)(\alpha P_{\ell,\beta} - L_{\ell,\beta}) \\ 2T_{\ell,\beta} \\ 2GX_{\ell} \end{pmatrix}, \quad \ell = 1, 2,$$

and $X_1 = P_{1,\beta}$, $X_2 = P_{2,\beta}$ for the case of boundary conditions (5), and $X_2 = 0$ for the impermeable boundary conditions (6).

1. *Вайсфельд Н. Д., Журавльова З. Ю.* Плоска змішана задача термопружності для півсмуги // Мат. методи та фіз.-мех. поля − 2015. − **58**, № 4. − С. 87−98.
    Translation: *Vaisfel'd N. D., Zhuravlova Z. Yu.* Two-dimensional mixed problem of thermoelasticity for a semistrip // J. Math. Sci. − 2018. − **228**, No. 2. − P. 105−121. − https://doi.org/10.1007/s10958-017-3609-8.
2. *Кубік Ю., Качмарик М., Чапля Є.* Про методи визначення характеристик пористих насичених середовищ // Фіз.-хім. механіка матеріалів. − 2021. − **37**, № 1. − С. 81−88.
    Translation: *Kubik J., Kachmaryk M., Chaplya E.* Methods for the determination of the characteristics of porous saturated media // Mater. Sci. − 2021. − **37**, No. 1. − P. 92−102. − https://doi.org/10.1023/A:1012342523893.
3. *Кушнір Р. М., Махоркін І. М., Махоркін М. І.* Аналітично-числове визначення статичного термопружного стану плоских багатошарових термочутливих структур // Мат. методи та фіз.-мех. поля. − 2019. − **62**, № 4. − С. 131−140.
    Translation: *Kushnir R. M., Makhorkin I. M., Makhorkin M. I.* Numerical-analytic determination of the static thermoelastic state of plane multilayer thermosensitive structures // J. Math. Sci. − 2022. − **265**, No. 3. − P. 498−511. − https://doi.org/10.1007/s10958-022-06067-5.
4. *Попов Г. Я., Вайсфельд Н. Д.* Точные решения некоторых краевых задач механики деформируемого твердого тела. − Одесса: Астропринт, 2013. − 423 с.
5. *Станкевич В. З., Михаськів В. В.* Інтенсивність динамічних напружень поздовжнього зсуву у періодично шаруватому композиті з круговими тріщинами // Мат. методи та фіз.-мех. поля. − 2020. − **63**, № 3. − С. 46−54. − https://doi.org/10.15407/mmpmf2020.63.3.46-54.
6. *Токовий Ю. В.* Розв'язки осесиметричних задач теорії пружності та термопружності для неоднорідних простору та півпростору // Мат. методи та фіз.-мех. поля. − 2017. − **60**, № 1. − С. 75−84.
    Translation: *Tokovyy Y. V.* Solutions of axisymmetric problems of elasticity and thermoelasticity for an inhomogeneous space and a half space // J. Math. Sci. − 2019. − **240**, No. 1. − P. 86−97. − https://doi.org/10.1007/s10958-019-04337-3.
7. *Biot M. A.* General theory of three-dimensional consolidation // J. Appl. Phys. − 1941. − **12**, No. 2. − P. 155−164. − https://doi.org/10.1063/1.1712886.
8. *Chebakov M. I., Kolosova E. M.* Contact interaction between parabolic punch and elastic strip bonded to poroelastic half-plane // I. A. Parinov, S. H. Chang, Y. H. Kim, N. A. Noda (eds.). Physics and Mechanics of New Materials and Their Applications: Proc. of the Int. Conf. PHENMA 2020. − Cham: Springer, 2021.− P. 321−330. − Ser.: Springer Proceedings in Materials. − Vol. 10. − https://doi.org/10.1007/978-3-030-76481-4_27.
9. *Cheng A. H.-D.* Poroelasticity. − Cham: Springer, 2016. − xxvi+877 p. − Ser.: Theory and Applications of Transport in Porous Media. − Vol. 27.
10. *Chopra M. B., Dargush G. F.* Dynamic response of embedded strip and rectangular foundations using a poroelastic BEM // WIT Trans. Modelling Simulation. − 1997. − 19. − 10 p.
11. *Gantmacher F. R.* The theory of matrices. − New York: Chelsea Publ. Co., 1959. − Vol. 1: x+377 p.; Vol. 2: x+277 p.
    Same: *Гантмахер Ф. Р.* Теория матриц. − Москва: Наука, 1966. − 576 с.
12. *He R., Zhang J., Guo Zh., Chen W.* Dynamic vertical and rocking impedances of a strip foundation in offshore engineering // Mar. Georesources Geotechnol. − 2021. − **39**, No 7. − P. 832−841. − https://doi.org/10.1080/1064119X.2020.1770907.

13. *Kovalenko M. D., Menshova I. V., Kerzhaev A. P., Yu G.* A strip with constant stresses on the cut: exact solutions // Z. Angew. Math. Mech. − 2022. − **102**, No. 10. − Art. e202100431. − https://doi.org/10.1002/zamm.202100431.

14. *Li P., Wang K., Lu D.* Analytical solution of plane-strain poroelasticity due to surface loading within a finite rectangular domain // Int. J. Geomech. − 2016. − **17**, No. 4. − Art. 04016089. − 8 p. − https://doi.org/10.1061/(ASCE)GM.1943-5622.0000776.

15. *Nahirnyj T., Tchervinka K.* Mathematical modeling of the coupled processes in nanoporous bodies // Acta Mech. Automat. − 2018. − **12**, No. 3. − P. 196−203. − https://doi.org/10.2478/ama-2018-0030.

16. *Terzaghi K.* Erdbaumechanik auf bodenphysikalischer Grundlage. − Wien: F. Deuticke, 1925. − 399 p.

17. *Theodorakopoulos D. D., Beskos D. E.* Flexural vibrations of poroelastic plates // Acta Mech. − 1994. − **103**, No. 1-4. − P. 191−203. − https://doi.org/10.1007/BF01180226.

18. *Selvadurai A. P. S., Samea P.* On the indentation of a poroelastic halfspace // Int. J. Eng. Sci. − 2020. − **149**. − Art. 103246. − https://doi.org/10.1016/j.ijengsci.2020.103246.

19. *Senjuntichai T., Keawsawasvong S.* Analytical methods for dynamic interaction between strip foundations and poroelastic soils // J. Reddy, C. Wang, V. Luong, A. Le (eds.).: Proc. of the Int. Conf. ICSCEA 2019. − Singapore: Springer, 2020. − P. 85−101. − Ser.: Lecture Notes in Civil Engineering. − Vol. 80. − https://doi.org/10.1007/978-981-15-5144-4_5.

20. *Senjuntichai T., Keawsawasvong S., Rajapakse R. K. N. D.* Vertical vibration of multiple flexible strip foundations on multilayered transversely isotropic poro− elastic soils // Int. J. Geomech. − 2021. − **21**, No. 11. − Art. 04021221. − https://doi.org/10.1061/(ASCE)GM.1943-5622.0002210.

21. *Shah S. A., Tajuddin M.* Three dimensional vibration analysis of an infinite poro− elastic plate immersed in an inviscid elastic fluid // Int. J. Eng. Sci. Tech. − 2011. − **3**, No. 2. − P. 1−11.

22. *Singh S. J., Rani S., Kumar R.* Quasi-static deformation of a poroelastic half-space with anisotropic permeability by two-dimensional surface loads // Geophys. J. Int. − 2007. − **170**, No. 3. − P. 1311−1327. − https://doi.org/10.1111/j.1365-246X.2007.03497.x.

23. *Vaysfeld N., Zhuravlova Z.* The plane problem of poroelasticity for a semi−plane // M. Abdel Wahab (ed.).: Proc. 4th Int. Conf. on Numerical Modelling in Engineering NME 2021. − Singapore: Springer, 2022. − P. 151−157. − Ser.: Lecture Notes in Mechanical Engineering. − https://doi.org/10.1007/978-981-16-8806-5_10.

24. *Verruijt A.* An introduction to soil dynamics. − Dordrecht: Springer, 2010. − xiv+433 p. − Ser.: Theory and applications of transport in porous media. − Vol. 24.

25. *Zheng C., Cai Y., Kouretzis G., Luan L.* Horizontal vibration of rigid strip footings on poroelasic half-space // J. Sound Vib. − 2022. − **552**. − Art. 116731. − https://doi.org/10.1016/j.jsv.2021.116731.

ВІДПОВІДЬ ПОРОПРУЖНОЇ НАПІВНЕСКІНЧЕННОЇ СМУГИ НА СТИСНЕННЯ УЗДОВЖ БІЧНИХ СТОРІН

З використанням теорії Біо сформульовано змішану крайову задачу для поропружної напівнескінченної смуги. Розглянуто два випадки крайових умов залежно від проникності довших сторін. Використовуючи інтегральні перетворення та матричне диференціальне числення, вихідну крайову задачу зведено до одновимірної, розв'язок якої знайдено аналітично. Отримано явні формули для ефективних напружень, порового тиску та переміщень. Проаналізовано залежності цих функцій проникності межі, властивостей пороеластичного матеріалу та профілю стисного навантаження на довших сторонах.

Ключові слова: поропружна півсмуга, інтегральне перетворення, матричне диференціальне числення, векторна крайова задача, точний розв'язок.

¹ King's college, London,
² Odesa I. I. Mechnikov National University, Odesa